Available online at www.sciencedirect.com
SCIENCE DIRECT®
Talanta 65 (2005) 54–61
Talanta
www.elsevier.com/locate/talanta

The role of rare earth elements and Mn^{2+} point defects on the luminescence of bavenite

J. Garcia-Guinea [a,*], V. Correcher [b], A. Quejido [b], A. LaIglesia [c], N. Can [d]

[a] *Museo Nacional de Ciencias Naturales. CSIC. José Gutiérrez Abascal 2 Madrid 28006, Spain*
[b] *CIEMAT. Avenida Complutense 22. Madrid 28040, Spain*
[c] *Instituto de Geología Económica. CSIC. Universidad Complutense Madrid 28040, Spain*
[d] *Physics Department, Faculty of Arts and Sciences, Celal Bayar University, 45030 Manisa, Turkey*

Received 10 November 2003; received in revised form 20 April 2004; accepted 12 May 2004

Abstract

Natural fibrous crystals of bavenite ($Ca_4Be_2Al_2Si_9O_{26}(OH)_2$) collected in intra-granitic pegmatite bodies of Bustarviejo (Madrid, Spain) have been examined by X-ray diffraction (XRD), scanning electron microscopy (SEM), electron microprobe (EMPA) and inductively coupled plasma–mass spectrometry (ICP–MS). The strong luminescence emissions of bavenite using thermoluminescence (TL), cathodoluminescence (CL) and its thermal stability have been recorded, looking for new physical properties and new phosphor or dosimetric uses. The bavenite luminescence takes place in the 5d electron shell that interacts strongly with the crystal field; the spectra bands assignment are Gd^{3+} (319 nm), Sm^{3+} (562 and 594 nm), Dy^{3+} (572 nm) and Tb^{3+} (495 nm). A Mn^{2+} band at about 578 nm in Ca^{2+} sites is present as a broad band that overlaps with the Dy^{3+}, Sm^{3+} and Tb^{3+} bands. Mn^{2+} is a transition metal ion that has an electron configuration of $3d^5$ and interacts strongly with the crystal field (d → d) transition. Stability tests at different temperatures show clearly that the TL glow curves at 400 nm in both irradiated and non-irradiated bavenite samples track the typical pattern of a system produced by a continuous trap distribution. The ICP–MS analyses show concentrations of Yb = 29.7 ppm, Dy = 22.7 ppm, Sm = 9.45 ppm, Nd = 8.95 ppm and Gd = 8.15 ppm in the bavenite lattice.

Keywords: Bavenite; Thermoluminescence; Cathodoluminescence; Point defects; Rare earth elements

1. Introduction

Cathodoluminescence (CL) spectroscopy is a promising technique for the analyses of trace element concentrations and distributions in minerals; in many cases, it also provides additional data, which cannot be obtained from backscattered electron image (BSE) or observing under the optical microscope [1]. The CL spectrometry can also be used as a microprobe studying activators in minerals; hence, it is important to note some inherent problems associated with the collection of the signals. These considerations are particularly relevant for mineralogical and geological applications, since for historical reasons the CL in these scientific areas often involves unfortunate practices such as earlier simplistic inter-comparisons of signals. A serious experimental problem is that diffraction gratings and photomultipliers vary considerably in efficiency as a function of wavelength. This system response implies modifications of the spectra in intensity and the shape of the bands [2]. Since these variations are strongly dependent on the impurity content of the samples, they will differ between specimens of the same material and between different zones of the same sample [3,4]. The variation in luminescence can be linked with crystallographic or electron beam aging [5]. The increased use of luminescence in environment radiation dosimetry and geological and archaeological dating has promoted interest in the causes of luminescence emissions of natural aluminosilicate minerals. Luminescence research on aluminosilicate phases have successfully linked to manganese and iron point defects with the 560 and 720 nm emissions in accordance with band theory models [6–10].

* Corresponding author. Tel.: +34 91 4111328; fax: +34 91 5644740.
E-mail address: guinea@mncn.csic.es (J. Garcia-Guinea).

0039-9140/$ – see front matter © 2004 Elsevier B.V. All rights reserved.
doi:10.1016/j.talanta.2004.05.016

The blue emission spectra of many Ca-rich silicates such as hsianghualite, datolite, damburite, hiortdalite and agrellite have been described in the reference book of Gorobets and Rogojine [9]; this book also includes radioluminescence spectra, at room temperature (RT) and liquid nitrogen temperature (LNT), of many other Be–Ca–silicates, such as bavenite, milarite, hsianghualite and leucophane formerly studied by Gorobets and Prokofiev [8]. For comparison, this bavenite radioluminescence (RL) spectra is here enclosed together with our experimental CL spectra plots. These CL plots of Spanish bavenite exhibit the same 316–319 nm peak observed by RL in Ca-rich silicates [9] and by laser-induced time-resolved luminescence also detected in other silicates such as orangite, xenotime, zircon, thorite and monazite [10]. In all cases, the emission is connected with Gd^{3+} centres in Ca^{2+} positions. Gd^{3+} has a half-filled 4f shell that gives a very stable $^8S_{7/2}$ ground state [10]. Furthermore, beryllium compounds, such as beryllium oxide display strong thermoluminescence (TL) and can be used as TL environmental dosimeters [11]. In short-radiation dosimetry, beryllium phases could have advantages such as commercial availability, low cost, chemical inertness, high sensitivity to ionizing radiations, good reproducibility of response, low fading, absence of low-temperature peaks and moderate energy dependence.

We found natural bavenite ($Ca_4Be_2Al_2Si_9O_{26}(OH)_2$) showing strong luminescence during a project on pegmatite minerals in the northern Madrid area of Bustarviejo. The granite pegmatite bodies have been studied previously describing minerals with unusual elements (Be, Nb, Ta, Ta, Sn, W, U, Y) and rare earth elements (REE) [12,13]. Bavenite is a rare, scarcely mentioned mineral [14,15] discovered in the Montecatini Quarry, Baveno, Piedmont, Italy [16], in very similar miarolitic cavities in the Baveno granite than in the Madrid case, i.e., calcium zeolites on post-pegmatitic minerals. Bavenite is an intermediate phase between chain and layered silicates of the prehnite series. In addition to REE, for thermoluminescence purposes, it is important to note the presence of hydroxyl groups in the bavenite formula, which take out during thermal pre-heating and TL analyses. Thermoluminescence glow curves from materials including hydroxyl groups (e.g., AlOOH, $Al_2Si_2O_5(OH)$, slate, etc.) display a continuous trap structure [17].

The aim of this study is to determine chemical composition (e.g., by electron microprobe (EMPA), inductively coupled plasma–mass spectrometry (ICP–MS)), texture, structure (X-ray diffraction (XRD), scanning electron microscopy (SEM)) and luminescent properties (TL, CL) of natural fibrous crystals of bavenite collected in a granitic pegmatite body of Bustarviejo (Madrid, Spain). Moreover, the work was focused to elucidate: (i) the huge luminescence of bavenite; (ii) the radically different behaviour of UV-blue and yellow spectra emissions in chemical mixed chalkalkali aluminosilicates as bavenite; (iii) the thermoluminescent emission in both irradiated and non-irradiated aliquots to determine its thermal stability and potential uses.

2. Sample and methodology

Bavenite fibrous samples were collected in a large rock cavity hosted in a pegmatite body in the granite massif of Bustarviejo (Madrid, Spain) (Fig. 1a and b). The habits of these bavenite crystals were observed under scanning electron microscopy (Fig. 1c); samples were coated with gold (20 nm) in a Bio-Rad SC515 sputter coating unit. SEM observations were performed in a Philips XL20 SEM at accelerating voltages of 20–30 kV. Energy-dispersive X-ray microanalyses (EDS) were obtained using a Phillips EDAX PV9900 with a light element detector type ECON. The structural data of bavenite aliquots was determined by X-ray powder diffraction using a Phillips PW1710/00 powder diffractometer with CuK_α radiation. Patterns were obtained by step scanning from 2′ to 64′ 20 in steps of 0.020′ with a count of 6 s per step and compared with the XRD Card file 13–535 (bavenite) of the Joint Committee on Powder Diffraction Standards. Measurements and refinement of cell parameters were performed with the PLV software created by J.D. Martin–Ramos of Granada (Spain), atomic positions were taken from the ICSD database and the structure was outlined with the crystal-builder software, i.e., Diamond 2.1e of Crystal Impact (Fig. 1d). The chemical composition of bavenite was determined by EMPA, optical emission analysis for Be and CHN analysis. REE was analyzed by a Finnigan MAT SOLA (Finnigan MAT, Bremen, Germany) plasma source mass spectrometer (ICP–MS). The sample was introduced into 27.12 MHz argon plasma using a Meinhard concentric nebulizer and a Gilson Minipuls 2 peristaltic pump. The instrument was calibrated using pure NIST traceable single-element stock solutions, supplied by Alfa (Alfa Products Ltd., Karlsruhe, Germany). Water and other reagents were prepared by sub-boiling procedure, except $HClO_4$ which was doubly quartz-distilled. The analysis of the rare earth elements of bavenite involves dissolving the sample in a mixture of HF and aqua regia. One gram of the sample was transferred to a PTFE closed vessel and 4 ml of concentrated HF and 2 ml of aqua regia were added. The vessel was kept overnight at 90 °C and, after cooling, the contents were transferred to a PTFE evaporating dish; 2 ml of concentrated $HClO_4$ was added and evaporated until white fumes were visible under an IR lamp. Finally, the residue was dissolved using diluted HNO_3 and the solution transferred to a 50 ml volumetric flask. To obtain these REE analyses, the ICP–MS equipment was previously calibrated using multi-elemental solutions containing all REE elements from 100- to 0.1-fold chondrite content. The isotopes were selected avoiding those affected by isobaric interferences from other REE elements or from La, Ce and Nd oxides, generated during ion formation.

Electron microprobe chemical analyses were carried out in a Jeol Superprobe JXA-8900M, with bulk and channel-selected (TAP, PETJ, LIF, PETH) X-ray spectra search and identification routines. We used the natural standards and synthetic crystals from the collection of the “Ser-

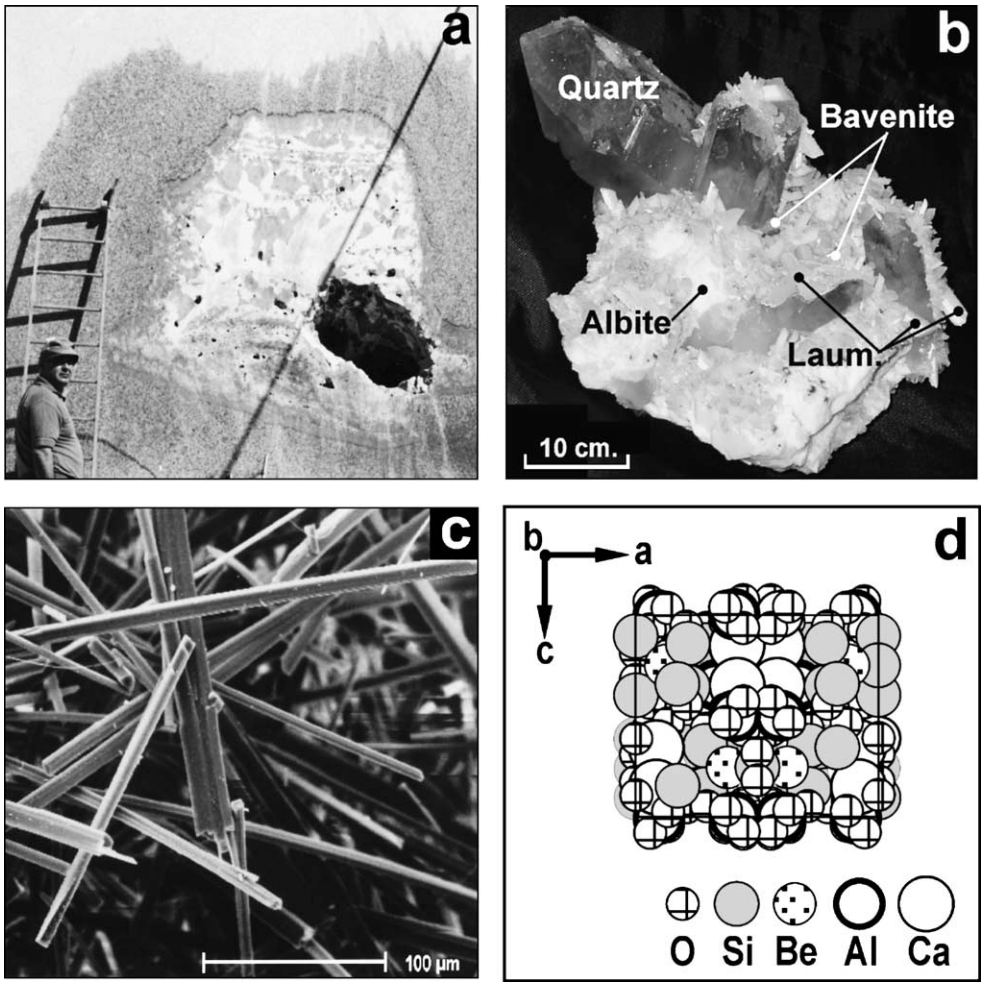

Fig. 1. Bavenite crystals: (a) fresh section of the ornamental granite rock (diamond wire cutting) showing both the pegmatite body and the natural pocket; (b) detail of the hydrothermal minerals which cover the internal walls of the cavity; (c) bavenite transparent needles under the scanning microscope; (d) Section (0 1 0) of the bavenite structure outlined with a crystal-builder software.

vicio de Microscopia Electronica Luis Bru", Complutense University, Madrid.

Cathodoluminescence spectra were excited using an electron beam of energy 14 keV focused into a spot 2 mm in diameter with a beam current 0.2–0.4 nA. It is worth noting that the broad diameter of the beam significantly reduces any instability due to secondary electron emission. The light coming from the sample was focused via a quartz lens onto the entrance slit of grating monochromator with f/4 light collection. Two different measurements were performed, namely alternative current (AC) and direct current (DC). In AC measurements, an Ortholo-SC9505 two-phase lock-in amplifier was employed. This instrument was used in normal mode where it performs in exactly the same way as an ordinary lock-in amplifier, i.e., only one channel is needed. Output from PM tube is first fed into a Brook-deal 5002 current pre-amplifier mounted near to the tube. This pre-amplifier provides a more suitable input to lock-in, being able to sink a considerable DC current. Its output can be varied to provide the optimum amount of AC gain against DC reduction. It makes a load resistor unnecessary and reduces the problem of noise pickup in the signal cable. Optical spectra were obtained using f/4 scanning monochromator, a cooled red sensitive photomultiplier output. The spectral coverage is 200–800 nm and the spectral dispersion is 2.8 nm mm^{-1} of slit width. The width of the entrance and exit slits is usually 1 mm, and therefore the spectral dispersion is 2.7 nm for the majority of the spectra presented in this work. Reducing the slits allows a better resolution, but produces an important decrease in the measured intensity. All spectra were recorded from the lower to higher wavelengths. The calibration of the wavelength and intensity was achieved with reference lamps whose emission spectra are known. Bausch & Lomb grating monochromator is calibrated with a low-pressure mercury vapour lamp with well-defined emission lines at 546.07, 576.96 and 579.06 nm. The monochromator can be driven mechanically to appropriate position, which enables precise acquisition data. The calibration of the apparatus can thus be easily controlled. To cover the entire range of the spectrum, two lamps whose spectra are broad bands with no line are needed. For the UV range (200–400 nm), a deuterium lamp whose spectrum corresponds to a broad band between 160

and 380 nm was used. Correction of a CL spectrum requires multiplication of the raw spectrum by the system response. All spectra shown here have been corrected for the system response. The electron beam was chopped at frequencies from 9 to 9 kHz and the photomultiplier output was measured on a lock-in amplifier. Modulation of the exciting electron beam has been accomplished by means of a pair of parallel plates inserted into the beam column. One advantage of a square wave may be that if the excitation beam is non-uniform, it still goes cleanly on and off the sample, rather than increase erratically as it sweeps into place. It may also influence the lower frequency limit as some of the harmonics will operate in the lock-in; similarly, there may be a disadvantage at high frequency with a square wave where the harmonics are above the working range. In DC measurement, the relatively high light intensities of the signals generated by the sample examined in this study made the more sophisticated techniques for detecting weak dc signals. In most cases, a dc signal was desirable, e.g., when there were strong lifetime effects at low-chopping rates, the signals were such that the background noise from the PM tube was negligible. Besides, the PM tube is fitted with an EMI FACT 50 cooling unit, and cooling to about $-15\,^{\circ}C$ is used before starting measurements. The advantages of doing this are that it diminishes the thermal noise by about 100 times relative to room temperature. Of greater importance for DC measurements proved to be the background due to the reflection at the sample of light from the gun filament. In cases where this forms a significant fraction of output, it can be subtracted using a computer after its contribution has been measured for each wavelength, by simply running a scan with the electron extraction voltage turned off. The CL response was studied as a function of intensities and wavelength or energy in both AC and DC measurements.

The TL measurements were carried out using an automated Risø TL system model TL DA-12; this reader is provided with an EMI 9635 QA photo-multiplier, and the bavenite emission was observed through a blue filter (FIB002) where the wavelength (in nm) peaked at 400 +25, −0; FWHM was 80 ± 16 nm and peak transmittance (minimum) was 60%. It also possesses a $^{90}Sr/Y$ source with a dose rate of $0.026\,Gy\,s^{-1}$ [18]. All the TL measurements were performed using a linear heating rate of $5\,^{\circ}C\,s^{-1}$ from room temperature up to 550 °C in an N_2 atmosphere. Four bavenite aliquots (5.0 ± 0.1 mg) were used for each measurement. Bavenite samples were carefully powdered with an agate pestle and mortar to avoid triboluminescence [19] and sieved to obtain a grain size fraction under 50 μm.

3. Results

3.1. Sample characterization

Bavenite transparent colourless crystals appear in a geode of ∼80 cm long, ∼70 cm wide and ∼80 cm high, and is studded with late-formed euhedral crystals, i.e., quartz, albite, epidote, prehnite, calcite, hematite and laumontite. Bavenite appears as cotton-like white masses covering these hydrothermal minerals (Figs. 1 and 2). Under the microscopes, i.e., under both optical and SEM (Fig. 1c), bavenite crystals show fragile prismatic-needle habits with a random three-dimensional orientation produced during the process of granite cutting and sample collection. The X-ray diffraction profile (powder method) of the Bustarviejo bavenite fits well with the bavenite 13–535 ASTM card, i.e., 3.71 Å (100%), 3.35 Å (90%), 3.22 Å (80%) and 11.6 Å (50%). Introducing 28 diffraction peaks in the PLV software, we refine the orthorhombic lattice, spatial group CMCM, obtaining the following cell parameters: a_o =23.11, b_o =4.98 and c_o =19.41. Using the bavenite Kharitinov 1971 entry of the ICSD database in a crystal-builder program to observe the 3-D views and draw round the structure (Fig. 1d). In addition, using a simple XRD sample heater [20] and operating in open air during 17 h is possible to observe minor reversible structural changes from RT to 100 °C, as annihilation and creation of the (1 3 1) crystallographic plane (Fig. 2). The chemical composition of major elements was determined by EMPA, optical emission analysis for Be and CHN; i.e., SiO_2 = 56.93%, Al_2O_3 = 10.47%, CaO = 23.78%, BeO = 9.6% and MgO = 0.01% The REE composition is shown in Table 1. The validation of the analytical method for REE was also performed analyzing three CRMs, containing low, medium and high REE contents. The concentrations obtained were normalized to chondrite concentrations [21] to detect LREE or HREE discrimination during bavenite mineralization. The REE concentration in bavenite, i.e., Yb = 29.7 ppm, Dy = 22.7 ppm, Sm = 9.5 ppm, Nd = 8.9 ppm, Gd = 8.1 ppm, Eu = 2.8 ppm and Ce = 5.3 ppm (Table 1) are in good agreement with the surrounding REE-bearing mineral parageneses, i.e., gadolinite, helvine, uraninite, thalenite, allanite, monazite, kainosite, vigezzite, ilmenite, cassiterite and xenotime [12,13].

Table 1
Chemical analysis of REE of the bavenite sample

Element	Final concentration (ppm)	Chondrite normalized concentration (ppm)
La	3.02	12.3
Ce	5.28	8.3
Pr	2.03	21.1
Nd	8.95	18.9
Sm	9.45	61.4
Eu	2.80	48.3
Gd	8.15	39.9
Tb	3.00	80.1
Dy	22.7	89.3
Ho	4.88	86.0
Er	13.1	78.9
Tm	3.02	117.9
Yb	29.7	179.6
Lu	6.75	265.9

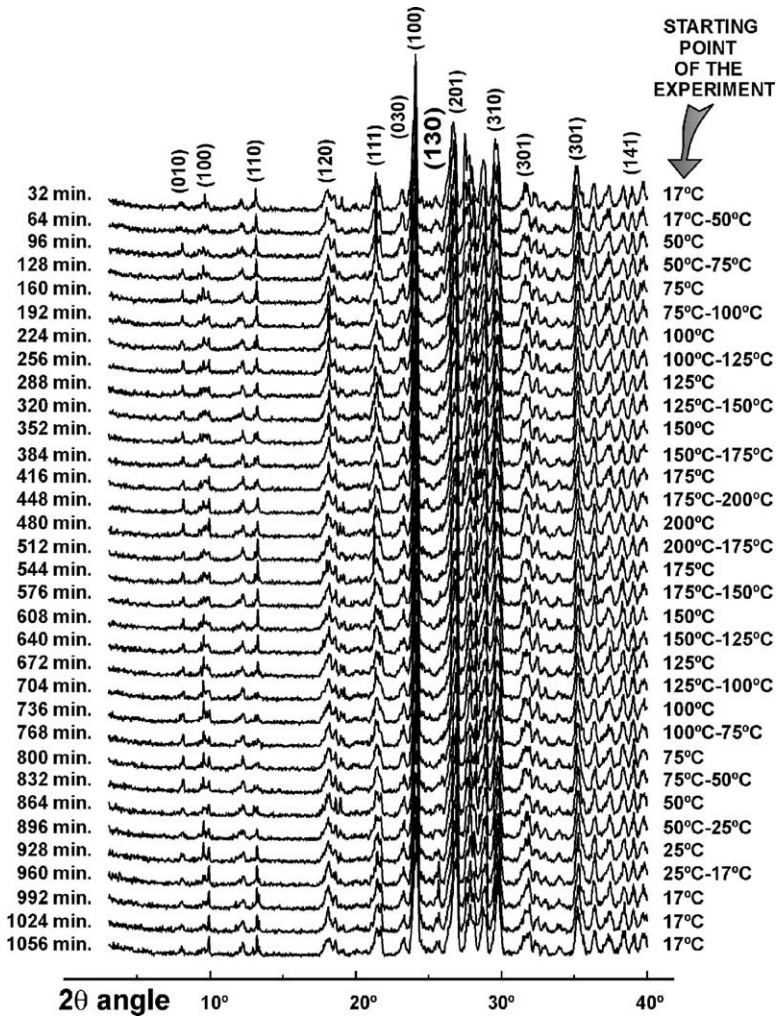

Fig. 2. Experiment using a self X-ray diffraction chamber to control the sample temperature.

3.2. Cathodoluminescence

Spectra CL of bavenite (AC measurements) display large difference between room and low temperatures and two different spectra regions at short wavelengths between 200 and 507 nm, i.e., UV-blue and long wavelengths between 507 and 800 nm, i.e., green-red-IR with a clear boundary at 507 nm (Fig. 3a). The thermal behaviour of both regions is dissimilar, as follows: (i) in the UV-blue region, at room temperature, bavenite displays an isolated peak at 319 nm and a broad band with a maximum peaked circa 374 nm and 1900 a.u.; conversely at cryogenic temperatures, this UV-blue emission grows up to 357 nm and 3800 a.u. keeping the 319, 352 and 373 nm spectra positions (Fig. 3a); (ii) in the green-IR region, at room temperature, bavenite shows a large isolated peak circa 578 nm of 14 000 a.u. while under the cryostat drops to 10 000 a.u. and shifts to 572 nm (see Fig. 3a). Spectra CL of bavenite (DC measurements) display similar results with a strong growing of circa four times of the UV-blue spectra band in cold conditions of sample in respect to the RT recordings (Fig. 3a). The Fig. 3a (down) shows RL spectra of a Russian bavenite at room and cold conditions taken from the Gorobets reference book [8], with a behaviour similar to that of the CL here presented (Fig. 3a top). In addition, it is important to note that in the UV-blue region, at higher frequencies of the electron gun (25 Hz), the broad band shows better defined peaks than that at lower frequencies, e.g., 5 Hz, Fig. 3b.

3.3. Thermoluminescence of bavenite pre-heated aliquots

The natural TL (NTL), i.e., light obtained from samples as a (received) response of bavenite (Fig. 4a) is very intense in comparison with other aluminosilicates, e.g., adularia, kaolinite, albite and microcline, measured under the same conditions. Natural bavenite samples reach light levels of $\sim 1.4 \times 10^6$ counts, whereas emissions of natural adularia ($KAlSi_3O_8$), natural kaolinite ($Al_2Si_2O_5(OH)_4$) or natural slates, i.e., mixtures of phyllosilicates, reach levels of ~500, ~14 000 and ~10 000, respectively [22]. Curves of NTL and induced TL glow curve by irradiation (ITL) were deconvoluted using both first order kinetic, i.e., where the intensity

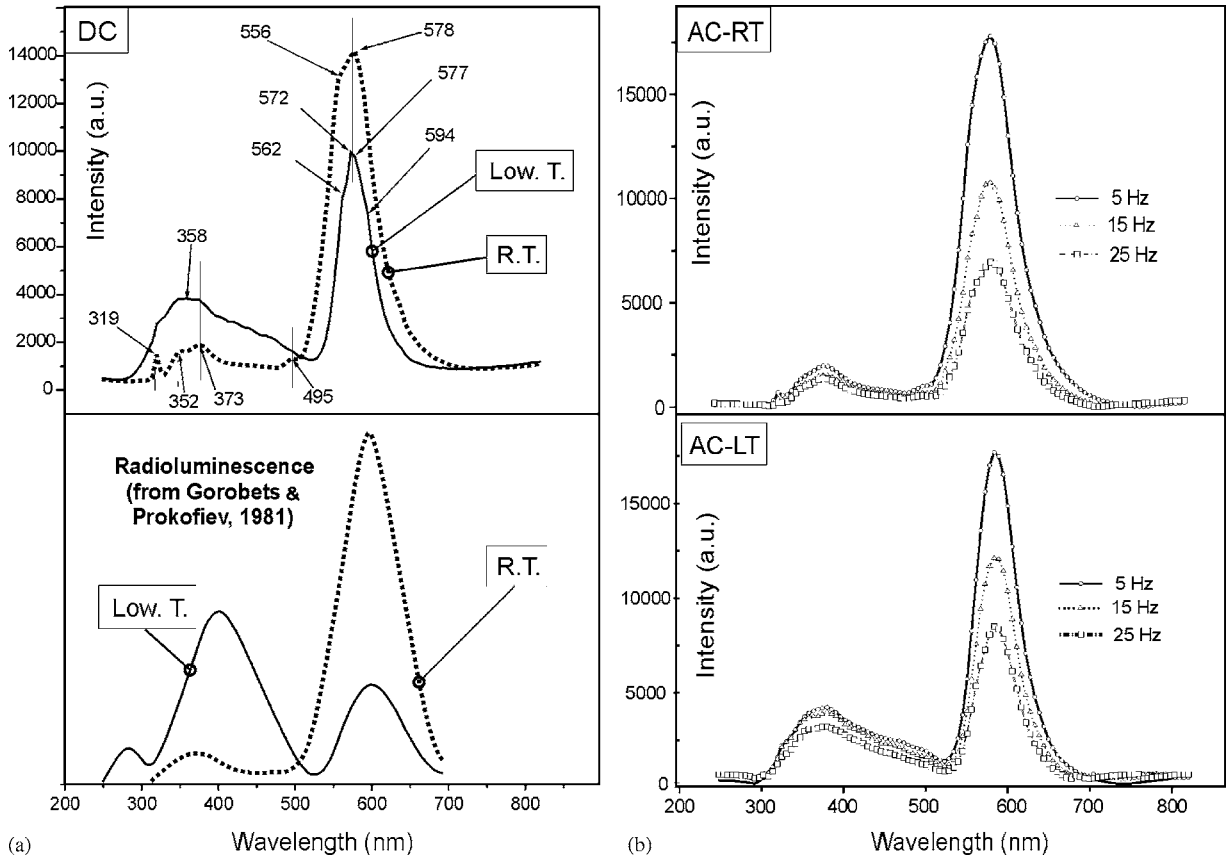

Fig. 3. A comparison of CL spectra from bavenite at room and low temperature for AC and DC measurements. The lock-in amplifier modulation frequencies were 5, 15 and 25 Hz. Although in arbitrary units, the scales are consistent. (Top-a), CL(DC) at RT and LT; (Down-a), bavenite radioluminescence adapted from Gorobets and Prokofiev [8]. (Top-b), CL(AC) at RT; (Down-b), CL(AC) at LT.

of the TL is proportional to the concentration of thermally released charges; and second order kinetic equations, i.e., the thermally released charges are retrapped at least once before the recombination process to determine the physical parameters. The fitting values obtained, which were based on the figure of merit, were not satisfactory. Therefore, as observed in the aforementioned aluminosilicates, the complexity in the shape of both NTL and ITL curves permits speculation on the possibility of a continuous trap distribution. The experimental was focused to determine the trap distribution of these bavenite samples, which can be confirmed by the evolution of the TL glow curve after progressive thermal treatments. Natural and irradiated bavenite samples were pre-heated ranging from 150 to 475 °C in 13 steps and from 60 to 340 °C in 11 steps, respectively, to test the response of the stability of the group of components after different sample pre-annealing (Fig. 4a and b).

4. Discussion

The first spectra band assignment for a bavenite collected in a beryllium-rich hydrothermal vein in Yermakovskoye, East Siberia, Russia, was proposed in 1981 by Gorobets and Prokofiev [9], i.e., Mn^{2+} in Ca^{2+} positions for the 600 nm peak and oxygen vacant for the 400 nm peak in good agreement with many other common aluminosilicates such as alkali feldspars. In the Spanish bavenite spectra case, two broad bands for bavenite, one centered at about 354 nm and other at about 578 nm, exist, and they can be explained in the same way. Furthermore, the CL spectra contain many other minor enclosed peaks, which could be linked with REE activators (Fig. 3). Bavenite Ca^{2+} positions are easily occupied by REE, Mn^{2+} and U^{4+}, very common in the paramagnetic surrounding minerals such as spessartine, uranium-opal and xenotime. These chemical exchanges were studied in chlorapatite crystals doped with various REE, Mn^{2+} and U^{4+} [22,23]. Trivalent rare earth ions have the electron configuration $4f^{(k)}$ [$5s^2 5p^6$], with the exceptions of La, Ce, Gd and Lu. The $5s^2 5p^6$ electrons form two completely filled shells, which partially shield the 4f subshell. These electron configurations give rise to characteristic luminescence bands through an f → f transition [24]. The interaction between 4f electron and the crystal field is weak, and therefore the emission band wavelengths vary with among different minerals [25]. Luminescence emission of trivalent rare earth elements can also take place in the 5d electron shell that interacts strongly with the crystal field, i.e., Gd^{3+} arising from the $^6P_{7/2}$ state (319 nm), Sm^{3+} arising from the $^4G_{5/2}$ state (562 and 594 nm), Dy^{3+} arising from $^4F_{9/2}$ state (572 nm)

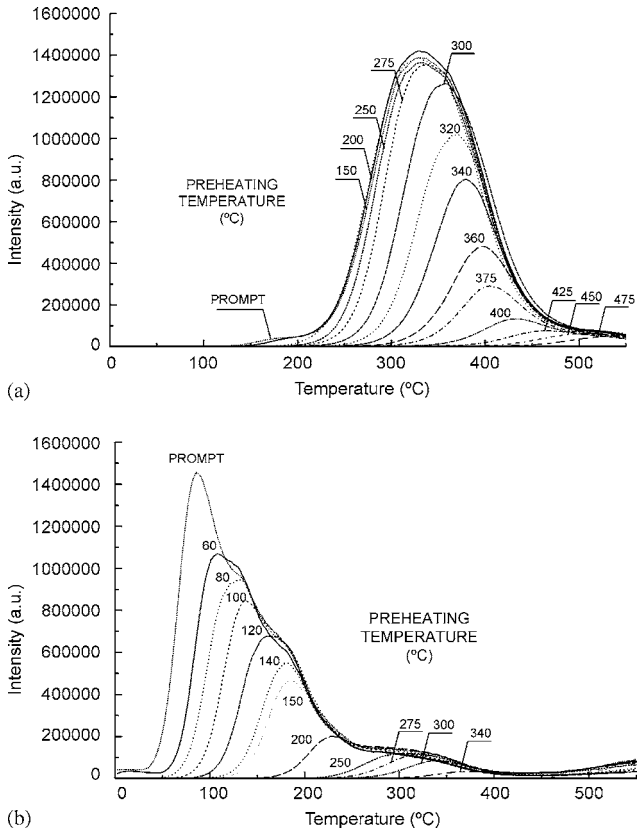

Fig. 4. Thermoluminescence glow curves of pre-heated bavenite at different temperatures: (a) non-irradiated and (b) 5 Gy beta irradiated.

and Tb^{3+} arising from the $^5D_3$ state (495 nm). A Mn^{2+} band at about 578 nm in M sites (most probably Ca^{2+} sites) is present as a broad band that overlaps with the Dy^{3+}, Sm^{3+} and Tb^{3+} bands. Mn^{2+} is a transition metal ion that has an electron configuration of $3d^5$ and interacts strongly with the crystal field (d → d) transition [26,10]. Most of the investigated alkali feldspars have Mn concentrations <10 ppm. There is no spectroscopic evidence to show which of the four calcium sites Mn^{2+} occupies in anorthite. Ce^{3+} activation has two bands at 352 and 373 nm [23]. In this study, we suggest that these two bands are related to Ce^{3+} activation. Introduction of Ce^{3+} ions in the apatite structure is claimed to produce vacancies or defects, and therefore to be associated with intrinsic luminescence [24].

The REE analyzed here by ICP–MS in the bavenite fibres are fairly well correlated with the mineral parageneses and rare earth elements previously described in these cavities in the pegmatite bodies of the plutonic granite of La Cabrera (Madrid) [13]. These bavenite samples have many chemical features probably involved with their strong luminescent spectra emissions as follows: (i) chemical mixing of chalk-alkali divalent elements (CaO = 23.78%, BeO = 9.6% and MgO = 0.01%) as in the alkali feldspar case; (ii) alkali cations (Na_2O = 0.05–0.09 and K_2O = 0.01–0.03); (iii) REE, Yb = 29.7 ppm, Dy = 22.7 ppm, Sm = 9.5 ppm, Nd = 8.9 ppm, Gd = 8.1 ppm, Eu = 2.8 ppm and Ce = 5.3 ppm; (iv) characteristic luminescent substitution ion centres, i.e., MnO = 0.01–0.02 and FeO = 0.02–0.06. The radically different behaviour of UV-blue spectra region and yellow CL spectra emissions is very common in other aluminosilicates such as feldspars [25,26]. The UV-blue luminescence is strongly dependent on the cryogenic stress exhibiting the classic features of other silicates such as the growing of the spectra region from 340 to 390 nm at LNT, which could also be raised to the chemical mixing of divalent elements (CaO, BeO and MgO) and the self-diffusion of little cations (Na^+ and Be^{2+}) through the lattice. The TL features shown in Fig. 4 typically involves the maximum peak shifting to higher temperatures and a change in the shape and intensity of the TL distribution in accordance with the specific thermal pre-treatment. This means that the luminescence process stems from a multiplicity of traps with different depths. The thermolabile broad band of blue emissions shows TL glow curves of multi-order kinetics involving continuous processes of trapping and detrapping. The response of this natural material to ionizing radiation after pre-heating (Fig. 4b) is less important in comparison to synthetic materials usually employed as dosimeters (TLD-100 -LiF:Mg, Ti- or GR-200 -LiF:Mg, Cu, Ti-), because (i) the presence of ionic charge compensators (Be^{2+}, Ca^{2+}, Na^+, K^+ or REE) is reduced, i.e., hole generation, during the heating treatment and (ii) structural modifications in the lattice, i.e., center destruction, could occur, decreasing the sensitivity during the luminescence processes after irradiation. Therefore, the production annihilation of luminescent $[AlO_4]^\circ$ centers can be analyzed in terms of both ionic self-diffusion (Be^{2+} and Ca^{2+}) and dehydroxylation heating beyond over 200 °C. As observed in Fig. 4a, prompt NTL and ITL glow curves of bavenite are quite different; an important change in the shape of the curves and the position of the main peaks can be observed. Thus, NTL consists of a low-intensity shoulder placed at ∼170 °C and a wide broad maximum peaked at ∼330 °C, whereas in ITL it is possible to distinguish, at least, three close groups of overlapping components at around 110, 140 and 180 °C, and at a higher temperature (∼330 °C), slightly separated from the another wider peak. The presence of light emission observed at low temperature in ITL is directly related to the radiation effect. The appearance of a very weak peak at 330 °C in ITL curves, i.e., in the same position than NTL, suggests that the bleaching effect induces movement of electrons from shallower to deeper traps linking the lower and higher temperature peaks in a photo-transfer process of these electrons [27]. This behaviour, observed in the TL glow curves of other natural materials and non-irradiated and irradiated bavenite, is interpreted as a continuous trap distribution.

5. Conclusion

The phenomenon of minerals luminescence has been known for a long time. Current works on lumines-

cence of minerals with their spectroscopic characteristics and interpretation have revealed new potentialities for luminescence in mineralogy. In this work, bavenite, ($Ca_4Be_2Al_2Si_9O_{26}(OH)_2$) displays a natural great luminescence, which takes place in the 5d electron shell that interacts strongly with the crystal field. The observed bands can be assigned as follows: Gd^{3+} (319 nm), Sm^{3+} (562 and 594 nm), Dy^{3+} (572 nm) and Tb^{3+} (495 nm). An Mn^{2+} band at about 578 nm in M sites (most probably Ca^{2+} sites) is present as a broad band that overlaps with the Dy^{3+}, Sm^{3+} and Tb^{3+} bands. Mn^{2+} is a transition metal ion that has an electron configuration of $3d^5$ and interacts strongly with the crystal field (d → d) transition. Stability tests at different temperatures show clearly that the TL glow curves at 400 nm, in both irradiated and non-irradiated bavenite samples, track the typical pattern of a system produced by a continuous trap distribution.

Acknowledgements

We are grateful to Prof. Dr. P.D. Townsend for the spectra cathodoluminescence measurements using the self-prototype, the University of Sussex (UK) and Rafael Gonzalez-Martin for the X-ray diffraction recordings of the sample. This work has been funded by the DGICYT PB95-0108-B and CICYT BFM2002-00048 projects.

References

[1] D.J. Marshall, Cathodoluminescence of Geological Materials, Unwin Hyman, Boston, p. 146.
[2] P.D. Townsend, A.P. Rowlands, Information encoded in cathodoluminescence emission spectra, in: M. Pagel, V. Barbin, P. Planc, D. Ohnenstetter (Eds.), Cathodoluminescence in Geosciences, Springer, Berlin, 2000, pp. 41–57.
[3] M.R. Krbetschek, J. Gotze, A. Dietrich, T. Trautmann, Rad. Meas. 27 (1998) 696.
[4] J. Gotze, Cathodoluminescence microscopy and spectroscopy in applied mineralogy, Freiberger Foschungshefte C485, ISBN 3-86012-116-2, 128 S, 2000.
[5] J.R. Murray, N. Oreskes, Econ. Geol. 92 (1997) 368.
[6] J.E. Geake, G. Walker, D.J. Telfer, A.A. Mills, Phil. Trans. R. Soc. Lond. A. 285 (1977) 403.
[7] D.J. Telfer, G. Walker, Mod. Geol. 6 (1978) 199.
[8] B.S. Gorobets, I.V. Prokofiev, Luminescence of minerals of beryllium, Izvestia AN SSSR (geol), 1981, p.117.
[9] B.S. Gorobets, A.A. Rogojine (Eds.), Luminescent Spectra of Minerals, ISBN 5-901837-05-3, VIMS, Moscow, 2002, 300 pp.
[10] M. Gaft, G. Panczer, R. Reisfeld, E. Uspensky, Phys. Chem. Miner. 28 (2001) 347.
[11] D.R. Vij, N. Singh, J. Mater. Sci. 32 (11) (1997) 2791.
[12] J. Gonzalez-Tanago, Rev. Soc. Geol. Esp. 10 (1997) 83.
[13] J. Gonzalez-Tanago, Estudios Geol. 54 (1998) 181.
[14] D.A.C. Manning, P. Putthapiban, S. Suensilpong, Min. Mag. 47 (342) (1983) 87.
[15] H.I. Micheelsen, E.S. Leonardsen, Neues J. Min-Mon. 7 (1995) 321.
[16] E. Artini, Atti Rendiconti Reale Accad Lincei Lincei 10 (1901) 139.
[17] J. Garcia-Guinea, J. Rubio, V. Correcher, F.J. Valle-Fuentes, Radiat. Meas. (2001) 653.
[18] V. Correcher, A. Delgado, Radiat. Meas. 29 (3–4) (1998) 411.
[19] J. Garcia-Guinea, V. Correcher, Spectrosc. Lett. 33 (2000) 103.
[20] J. Garcia-Guinea, R. Ortiz, V. Correcher, A. LaIglesia, J.D. Martín-Ramos, Rev. Sci. Instrum. 72 (10) (2001) 4005.
[21] N.M. Evensen, P.J. Hamilton, R.K. O'Nions, Geochim. Cosmochim. Acta 42 (1978) 1199.
[22] V. Correcher, J. García-Guinea, A. Delgado, Radiat. Meas. 32 (2000) 709.
[23] P.H. Blanc, A. Baumer, F. Cesbron, D. Ohnenstetter, Compte Rendu de l'Academie des Sciences Paris 321 (1995) 1119.
[24] J. Barbarand, M. Pagel, Am. Miner. 86 (2001) 473.
[25] R.J. Brooks, A.A. Finch, D.E. Hole, P.D. Townsend, Contrib. Miner. Petrol. 143 (2002) 484.
[26] A.A. Finch, D.E. Hole, P.D. Townsend, Phys. Chem. Miner. 30 (6) (2003) 373.
[27] J.R. Prescott, P.J. Fox, G.B. Robertson, J.T. Hutton, Radiat. Meas. 23 (1994) 367.